



# HHS Public Access

Author manuscript

*Nat Struct Mol Biol.* Author manuscript; available in PMC 2010 September 01.

Published in final edited form as:

*Nat Struct Mol Biol.* 2010 March ; 17(3): 332–338. doi:10.1038/nsmb.1770.

## A distinct mechanism for the ABC transporter BtuCD-F revealed by the dynamics of complex formation

Oded Lewinson<sup>1</sup>, Allen T. Lee<sup>1,2</sup>, Kaspar P. Locher<sup>3</sup>, and Douglas C. Rees<sup>1,2</sup>

<sup>1</sup> Division of Chemistry and Chemical Engineering, California Institute of Technology Pasadena, CA 91125, USA <sup>2</sup> Howard Hughes Medical Institute California Institute of Technology Pasadena, CA 91125, USA <sup>3</sup> Institute of Molecular Biology and Biophysics ETH Zurich, 8093 Zurich, Switzerland

### Abstract

ATP binding cassette (ABC) transporters are integral membrane proteins that translocate a diverse array of substrates across cell membranes. We present here the dynamics of complex formation of three structurally characterized ABC transporters: the BtuCD vitamin B<sub>12</sub> importer and MetNI D/L-methionine importer from *Escherichia coli*, and the *Haemophilus influenzae* Hi1470/1 metal-chelate importer, with their cognate binding proteins. Similar to other ABC importers, MetNI interacts with its binding protein with low affinity ( $K_d \sim 10^{-4}$  M). In contrast, BtuCD-F and Hi1470/1-2 form stable, high affinity complexes ( $K_d \sim 10^{-13}$  and  $10^{-9}$  M, respectively). In BtuCD-F, vitamin B<sub>12</sub> accelerates complex dissociation rate  $\sim 10^7$ -fold, with ATP having an additional destabilizing effect. The findings presented here highlight substantial mechanistic differences between BtuCD-F, and likely Hi1470/1-2, and the better characterized maltose and related ABC transport systems, indicating considerable mechanistic diversity within this large protein super-family.

### Introduction

ATP Binding Cassette (ABC) transporters are a ubiquitous super-family of proteins present in all kingdoms of life<sup>1,2</sup>. These transporters couple the energy of ATP hydrolysis to the translocation of a diverse array of substrates across biological membranes. A large body of experimental evidence supports a “two-state, alternating access” mechanistic model for ABC exporters and importers<sup>3-6</sup>. In this model, ATP binding, hydrolysis, and product release drive the conformational changes of the transporter between two major conformations: an outward-facing conformation, in which the substrate-binding site is exposed to the extracellular side of the membrane, and an inward-facing conformation that

Users may view, print, copy, download and text and data- mine the content in such documents, for the purposes of academic research, subject always to the full Conditions of use: [http://www.nature.com/authors/editorial\\_policies/license.html#terms](http://www.nature.com/authors/editorial_policies/license.html#terms)

Corresponding author: Douglas C. Rees. [dcree@caltech.edu](mailto:dcree@caltech.edu); telephone: 626-395-8393; fax: 626-744-9524.

Author contributions.

A.L. and K.P.L. generated the original constructs used in this work, O.L. and D.C.R. designed the research; O.L. and A.T.L. performed the research; O.L., A.T.L., K.P.L., and D.C.R. analyzed the data; and O.L., K.P.L. and D.C.R. wrote the paper.

The authors declare no conflict of interest.

exposes the binding site to the cytoplasm. Concerted with changes in the affinity of the binding site towards the substrate, these conformational changes ensure net substrate uptake by an importer, or net expulsion by an exporter.

ABC transporters that import essential nutrients into cells depend on a high affinity binding protein for their function<sup>7-9</sup>. The binding protein acts as a substrate chaperone that shuttles back and forth from the periplasm to the transporter to deliver substrate molecules. The integration of the binding protein into the above-mentioned “two-state” model is such that a substrate-loaded binding protein associates with the ATP-bound transporter, thus facilitating closure of the nucleotide binding domains and stabilizing the outward facing conformation<sup>10,11</sup>. ATP hydrolysis and subsequent phosphate release drive a conformational change to the inward-facing conformation, followed by substrate release, and dissociation of the transporter/binding protein complex. This scheme of events is perhaps best exemplified by the maltose transporter, as has been comprehensively demonstrated by Davidson, Chen and colleagues<sup>4</sup>.

In *Escherichia coli* and other gram-negative bacteria, vitamin B<sub>12</sub> transport across the outer membrane is mediated by the collaborative action of a high affinity,  $\beta$ -barrel type outer membrane transporter BtuB, and TonB, a periplasmic protein<sup>12,13</sup>. Once vitamin B<sub>12</sub> accumulates in the periplasm, its passage through the inner membrane depends on the action of BtuCD, the *E. coli* vitamin B<sub>12</sub> ABC transporter, and BtuF, its high affinity cognate substrate-binding protein<sup>14</sup>. Several observations in the *E. coli* vitamin B<sub>12</sub> ABC transport system are suggestive that BtuCD-F operates by a distinctive mechanism relative to that established for the maltose transporter and related ABC transporters. The vitamin B<sub>12</sub> binding protein, BtuF, has been demonstrated to form an extremely stable complex with BtuCD<sup>15,16</sup>. Such an essentially irreversible interaction is inconsistent with a mechanism in which the binding protein associates and dissociates from the transporter during each transport cycle. In addition, upon ATP binding, an EPR spin label attached to the cytoplasmic gate showed increased mobility<sup>17</sup>. Although this observation does not provide direct proof, it is compatible with opening of this gate to the cytoplasm upon ATP binding.

To better characterize the mechanism of vitamin B<sub>12</sub> transport, we have studied in detail the dynamic nature of association and dissociation between BtuCD (the transporter) and BtuF (the binding protein) using Surface Plasmon Resonance (SPR, or BiaCore™). We have complemented these studies with several other experimental approaches and in the present report we delineate the kinetic and energetic relationships characterizing the interactions between the transporter, binding protein and substrate. The results indicate that BtuCD operates by a distinct mechanism than that proposed for the maltose transporter and related ABC transporters. We propose that ABC importers can be divided into groups that differ not only phylogenetically<sup>4,18</sup> and structurally<sup>5,19</sup>, but also mechanistically. We support this hypothesis with preliminary characterization of two additional structurally characterized ABC import systems: the D/L-methionine transporter MetIN-Q, and the metal-chelate transporter Hi1470/1-2.

## Results

### Association between importers and their binding proteins

Models of binding protein dependent ABC transporters depict a short-lived association between the transporter and its soluble binding protein, in which the binding protein shuttles between the periplasm and the transporter to deliver substrate molecules. However, the association between the vitamin B<sub>12</sub> transporter BtuCD and its binding protein, BtuF, does not fit this model. As demonstrated by gel filtration experiments, when BtuF is prepared in the absence of substrate and then mixed with BtuCD at a 1:1 molar ratio, virtually all BtuF is in complex with the transporter, and none can be detected in free form (Fig 1a). This complex can then be isolated, and is extremely stable<sup>16</sup>. Similar results were obtained with the *Haemophilus influenzae* putative metal-chelate ABC import system, Hi1470/1-2. Prior to injection, a 1:1 molar ratio incubation of this transporter with its binding protein results in a shift in the location and an increase in area of the transporter peak, accompanied by an almost complete disappearance of the binding protein peak (Fig 1b). In contrast to these two observations, yet similar to what has been reported for the maltose and histidine uptake systems, no complex formation was observed in the methionine uptake system, even when the transporter (MetIN) was present at a 5-fold, 10-fold, or 20-fold molar excess of the binding protein (MetQ; Fig 1c and not shown).

Surface Plasmon Resonance (SPR or BiaCore™) was used to further characterize the interactions between ABC transporters and their binding proteins. BtuCD, Hi1470/1, and MetIN were immobilized via His-tags on a BiaCore chip. Following immobilization, non His-tagged binding proteins (BtuF, Hi1472, or MetQ, respectively) were injected onto the flow cells. Figure 2a-c demonstrates the specificity of the BiaCore system, as the transporters interacted only with their cognate binding proteins, and not with binding proteins from different systems. When 20 nM BtuF is flowed over a flow cell onto which BtuCD is immobilized, a robust response, representing complex formation is measured (Fig. 2a). Once the injection is terminated (and washing of the chip with buffer begins), the complex is stable and does not dissociate. Similarly, upon injection of 20 nM Hi1472 over immobilized Hi1470/1, the two rapidly associate, and complete dissociation is observed only after 30-40 min (Fig. 2b). A much higher concentration (15 μM) was necessary to elicit a proportional response when injecting MetQ over immobilized MetIN. In this system, complex formation is also observed (Fig. 2c); however, in contrast to the previous two transport systems, upon termination of MetQ injection (and commencement of chip washing with buffer), the MetIN-Q complex quickly dissociates. The different kinetic behavior of the three import systems is further illustrated in Fig. 2d-f, where a series of concentrations of the binding proteins is injected over a constant concentration of the transporters.

The association/dissociation curves of all three systems displayed clear biphasic characteristics, and were better described by applying fitting models that take into account a possible conformational change upon association (see the methods section). The initial association event ( $k_{a1}$  values in Table I) of the three import systems is characterized by moderate to fast rates ( $\sim 10^3$  to  $10^5$  M<sup>-1</sup>s<sup>-1</sup>), with Hi1470/1/2 being the fastest, and MetIN-Q the slowest. As can be appreciated by a visual comparison of Fig. 2 c-f, greater variance is

observed in the dissociation rates. While the  $k_{d1}$  for BtuCD-F is almost negligible at  $\sim 10^{-8} \text{ s}^{-1}$  (i.e.  $\sim 2 \times 10^{-3} \text{ day}^{-1}$ ), the corresponding value for MetIN-Q,  $\sim 0.2 \text{ s}^{-1}$  (Table I), is compatible with measured transport rates of ABC transporters<sup>20,22</sup>. Derivation of the equilibrium dissociation constants ( $K_d$ ) from the rate constants given in Table I yield high ( $10^{-13} \text{ M}$ ), medium ( $\sim 10^{-9} \text{ M}$ ), and low ( $10^{-4} \text{ M}$ ) affinities for BtuCD-F, Hi1470/1/2 and MetIN-Q, respectively. The  $\sim 100$  micromolar  $K_d$  ( $7.4 \times 10^{-5} \text{ M}$ ) of the MetIN-Q interaction is in agreement with its anticipated low affinity, as suggested by the gel filtration results (Fig. 1c). Similarly low affinities were measured in the maltose, histidine and oligopeptide systems<sup>9,23,24</sup>. While the  $k_{a1}$  for the three studied systems differ by two orders of magnitude, the  $k_{d1}$  and equilibrium constants vary by up to 8 orders of magnitude (Table 1), indicating that the dominant contributions to changes in binding affinities reflect variations in the dissociation rate constants.

To study whether a high-affinity BtuCD-F complex also forms in the membrane milieu, BtuCD was reconstituted into liposomes. The interaction of BtuCD-liposomes with BtuF was then compared to the interactions of BtuF with either empty liposomes or liposomes reconstituted with MetIN. BtuF (20 nM) was added to liposomes or proteoliposomes containing equal amounts of either BtuCD or MetIN. Following a 10-minute incubation, the liposomes were pelleted by ultracentrifugation. As shown (Fig 2g), most, if not all of the added BtuF was bound to the BtuCD-liposomes, while none was found to associate with either the MetIN-liposomes or the empty liposomes. In contrast, no unbound BtuF was detected in the soluble fraction of the BtuCD-liposomes, and all of BtuF was found in the soluble fractions of the MetIN-liposomes and the empty liposomes. The seemingly complete binding of BtuF by BtuCD-liposomes is indicative that the  $K_d$  of the interaction is lower than 20 nM. Lower BtuF concentrations could not be tested since 20 nM is the detection limit of this SDS-PAGE-based assay (see methods).

### Vitamin B<sub>12</sub> binding and release

The stability of the transporter-binding protein complex, characteristic of the vitamin B<sub>12</sub> and Hi1470/1-2 uptake systems, prompted speculations that perhaps it is this complex that is responsible for substrate binding<sup>20</sup>. Vitamin B<sub>12</sub> forms a pinkish aqueous solution with an absorbance maximum at 360 nm, which enables detection of its association with proteins. BtuCD, BtuF and the complex BtuCD-F were purified to homogeneity and analyzed by size exclusion chromatography before (Fig. 3a) or after (Fig. 3b) incubation with vitamin B<sub>12</sub>. When BtuCD is incubated with 50  $\mu\text{M}$  vitamin B<sub>12</sub>, no 360 nm absorbance is observed in the fractions corresponding to the 280 nm elution peak of the transporter. Additions of ATP/Mg, ADP/Mg, AMP-PNP/Mg, AMP-PCP/Mg or ATP/EDTA (see methods for details) yielded identical 360 nm elution profiles, suggesting that regardless of its nucleotide state, BtuCD does not bind vitamin B<sub>12</sub> with high affinity at the tested concentration range (10-100  $\mu\text{M}$ ). Much like the free transporter, the BtuCD-F complex does not bind vitamin B<sub>12</sub> (Fig. 3b), irrespective of the nucleotide state of the transport complex. In contrast to BtuCD or the complex BtuCD-F, when the periplasmic binding protein BtuF is prepared in the absence of vitamin B<sub>12</sub>, and then incubated with this substrate, the two associate tightly as indicated by the 360 nm peak eluting at  $\sim 17 \text{ ml}$ , and by the decrease in the amount of free vitamin B<sub>12</sub> eluting at  $\sim 20.5 \text{ ml}$ . These results are in agreement with the reported high

affinity (~15 nM) of BtuF to B<sub>12</sub><sup>14</sup>. Taken together, these results suggest that only free, un-complexed BtuF binds substrate with high affinity, while the free transporter, or the transport complex, lack this capacity regardless of their nucleotide state.

A similar approach was employed to investigate substrate release in the BtuCD-F transport system. In these experiments, the binding protein (BtuF) was prepared in the presence of a saturating concentration (10 μM) of vitamin B<sub>12</sub>. Figure 4a shows the 360 nm elution profile when such a preparation is submitted to gel filtration chromatography. Two clear peaks can be distinguished: one eluting at ~17 ml and the other eluting at ~20.5 ml. These two peaks correspond to BtuF-bound vitamin B<sub>12</sub> and free vitamin B<sub>12</sub>, respectively. When the same preparation is subjected to a 10-fold or a 100-fold wash with buffer devoid of vitamin B<sub>12</sub> (see methods for details), the latter peak diminishes and all but disappears, while the peak corresponding to the BtuF-bound vitamin B<sub>12</sub> remains almost constant (Fig. 4a). This observation suggests that under these conditions, vitamin B<sub>12</sub> is not efficiently released from BtuF. When an identical preparation of vitamin B<sub>12</sub>-loaded BtuF (washed 100-fold from any free vitamin B<sub>12</sub>) is mixed with BtuCD at a molar ratio of 1:2 (BtuCD:BtuF), roughly half of the 360 nm signal previously associated with BtuF appears as free vitamin B<sub>12</sub> (Fig. 4b, red trace). When vitamin B<sub>12</sub>-loaded BtuF is mixed with BtuCD at a 1:1 molar ratio, almost all of the vitamin B<sub>12</sub> appears in free form. Addition of BtuCD in excess of BtuF (2:1 molar ratio) results in complete release of vitamin B<sub>12</sub> from BtuF (Fig. 4b, compare 20.5 ml peak of green trace and ~17 ml peak of cyan trace, respectively). The small 360 nm peak that gradually appears at ~13.5 ml reflects the small absorbance that BtuCD and the BtuCD-F complex have in this wavelength. Vitamin B<sub>12</sub> was never observed to associate with either BtuCD or the complex BtuCD-F, suggesting that upon binding of BtuF to BtuCD, vitamin B<sub>12</sub> is released from BtuF, and is only transiently associated with the complex.

### Substrate effects on the association between BtuCD and BtuF

The effect of substrate on complex formation was investigated through BiaCore experiments where BtuF was injected in the presence of increasing concentrations of vitamin B<sub>12</sub> (Fig. 5a). Remarkably, the stability of the BtuCDF complex was observed to decrease in the presence of vitamin B<sub>12</sub>. So pronounced was this effect, that in the presence of vitamin B<sub>12</sub> concentrations >50 μM, the equilibrium affinity decreases by ~5 orders of magnitude (Table I). In Fig. 5a, the greatest effect of increasing the vitamin B<sub>12</sub> concentrations was between 0.48 μM and 2.4 μM. This is most probably due to the degree of occupancy of BtuF (1 μM used in this experiment) by vitamin B<sub>12</sub>, rather than the binding affinity of BtuF towards vitamin B<sub>12</sub>.

Two additional, independent experimental methods were employed to validate this observation. In the first set of experiments, size exclusion chromatography was used to qualitatively evaluate the effect of substrate on complex formation. Fig. 5b shows that when BtuF is prepared in the absence of substrate and then incubated with a two-fold molar excess of BtuCD, no peak representing free BtuF is observed, and practically all of the binding protein is associated with the transporter. When 100 μM vitamin B<sub>12</sub> is added to BtuF prior to its incubation with BtuCD, all the BtuF appears as a free, un-complexed form (compare ~17 ml peak of red and green traces in Fig. 5b). Similar results were obtained by pull-down

experiments, where either His-tagged BtuCD or His-tagged BtuF were immobilized on Ni-NTA beads and incubated with a FLAG-tagged partner (see methods for details). Fig. 5c shows that also in these experiments, the amount of retained FLAG-tagged protein was inversely related to the concentration of vitamin B<sub>12</sub>. As observed in the BiaCore system (Fig. 5a), the greatest effect of the increasing vitamin B<sub>12</sub> concentrations was between 233 nM and 2.85 μM, reflecting the BtuF concentration (~2 μM) used in this experiment.

Substrate effects were also studied in a liposome-reconstituted system. In these experiments, 35 nM BtuF were added to BtuCD-liposomes in the presence or absence of various concentrations of vitamin B<sub>12</sub>. Similar to what has been observed in the solution experiments (Biacore, gel-filtration, pull-downs), the affinity between BtuCD and BtuF decreased with increasing substrate concentrations (Fig. 5d).

To further characterize the observed substrate effects, rate constants of complex association and dissociation were determined in the presence of saturating vitamin B<sub>12</sub> concentrations. Relative to the values determined in the absence of substrate, addition of substrate resulted in a modest (10-20-fold) stimulation of  $k_{a1}$  (Fig. 6a, Table 1). However, most remarkable is the substrate-induced stimulation of complex dissociation: in the presence of vitamin B<sub>12</sub>, the  $k_{d1}$  of the initial interaction is accelerated by ~8 orders of magnitude, from  $1.12 \times 10^{-8} \text{ s}^{-1}$  to  $1.55 \text{ s}^{-1}$  (Fig. 2d, Fig. 6a, Table 1). The equilibrium dissociation constant ( $K_d = 2.11 \times 10^{-8} \text{ M}$ ) calculated between the binding protein and transporter in the presence of vitamin B<sub>12</sub> is consistent with the substrate-induced decrease in equilibrium affinity described above (Fig. 5).

### Effects of nucleotide on BtuCD-F association/dissociation

The effects of nucleotide binding and hydrolysis on the interactions between BtuCD and BtuF were measured at several conditions that presumably mimic the sequential steps of ATP hydrolysis. Binding of nucleotides by BtuCD and BtuCD-F was verified by measuring the 260/280 nm absorbance ratios in the absence or presence of ATP, and by conducting ATP hydrolysis assays (see supplementary methods and supplementary Fig. 1). Notably, in the presence of vitamin B<sub>12</sub>, upon binding of ATP (or ATP analogues), no association between BtuF and BtuCD could be detected (Compare Fig. 6a and 6b). The reduced affinity between the nucleotide bound transporter and the substrate-loaded binding protein was also observed in pull-down experiments. Using this approach, complex formation was readily observed in the nucleotide-free state, yet was undetectable in the nucleotide-bound state (Fig. 6b inset). Importantly, the lack of interaction between BtuCD and BtuF was not due to any destabilizing effects of nucleotide binding on BtuCD (supplementary Fig. 2).

The combined effect of substrate and nucleotide binding was also studied in the liposome-reconstituted system. In these experiments, BtuCD-reconstituted liposomes were prepared in the presence or absence of 1 mM ATP, 50 μM EDTA. As shown (Fig. 6f), ATP binding by membrane-embedded BtuCD decreased its affinity to BtuF both in the absence or presence of substrate. Such was this effect, that in the presence ATP, EDTA, and saturating concentrations of vitamin B<sub>12</sub>, no complex formation could be detected.

Concomitant additions of ATP, magnesium, and vanadate have previously been used to trap ABC transporters<sup>25,26</sup> and BtuCD (<sup>20</sup> and supplementary Fig. 1) in a transition state of ATP hydrolysis. Similar to what has been observed in the nucleotide-bound state, in the presence of vitamin B<sub>12</sub>, no complex formation could be detected in this transition state (Fig. 6c). Interestingly, in the maltose ABC import system, this state induces the highest affinity between the maltose transporter and the maltose binding protein<sup>21,27</sup>. It seems that the opposite is true for the vitamin B<sub>12</sub> ABC transport system.

The post-hydrolysis, ADP-bound state is shown in Fig. 6d. In this state, complex formation and dissociation are once again readily detected with kinetic constants that are similar to the nucleotide-free state (Table 1).

Generation of hydrolytic conditions by addition of Mg-ATP likely results in a mixed population of BtuCD molecules as they progress through the various conformations accompanying ATP binding and hydrolysis. This ensemble of conformations is comprised of four of the above-mentioned states (Fig 6a to 6d). Thus, the kinetic parameters measured under hydrolyzing conditions are a weighted average, dictated by the proportion of the molecules residing at each state, and the average dwell time in each state. Fig 6e shows a sensogram recording in the presence of vitamin B<sub>12</sub> and Mg-ATP, with rate constants that are most similar to those determined in the absence of nucleotide or in the presence of Mg-ADP (Table 1). Considering the high levels of cellular ATP, this suggests that on average, ATP-hydrolyzing BtuCD molecules reside longer in the ADP-bound state than in the pre-hydrolysis (ATP bound) or in the transition (Mg-ATP/vanadate) states, where no association was observed.

## Discussion

In the present report, we have studied in detail the effects of substrate and nucleotide binding on the formation of the BtuCD-F vitamin B<sub>12</sub> transport complex. As discussed below, a synopsis of the current data suggest a distinct mechanism of transport in this system relative to the model developed for the more extensively characterized maltose ABC transporter.

In the absence of vitamin B<sub>12</sub>, BtuF at concentrations above 10<sup>-11</sup> M, will be bound by BtuCD. Our previous<sup>20</sup> and current (supplementary figure 1) results indicate that the BtuCD-F complex binds and hydrolyzes ATP at least as efficiently as free BtuCD, both in proteoliposomes and in solution. We expect this substrate-free complex to shift through the energetic minima depicted in the bottom left corners of panels I-IV of the thermodynamic scheme shown in Fig. 7a. The high intrinsic stability of the complex presents a considerable energetic hurdle for productive transport: the crystal structure<sup>16</sup> of BtuCD-F indicates that once the complex has formed, vitamin B<sub>12</sub> cannot access the binding site. This notion is supported here by the observation that the complex is unable to bind substrate (Fig. 3). Hence, the complex must dissociate for transport to occur (Fig. 7b state I). As shown (Figs 5 and 6), complex dissociation is facilitated by both substrate and ATP. However, other factors may also affect the association of BtuCD and BtuF. For example, through its interaction with BtuF, TonB<sup>28</sup> may influence the formation of the BtuCD-F complex. In

addition, tight transcriptional and/or translational control (as have been observed in the vitamin B<sub>12</sub> uptake system and related systems<sup>29,31</sup>) may prevent expression of BtuCD-F in the absence of substrate. Clearly, further studies are required to resolve these complexities.

As vitamin B<sub>12</sub> is transported into the periplasm by BtuB and TonB, it can only be efficiently bound by BtuF, which is the only component of the system with high substrate affinity<sup>14</sup> (Fig 3). Neither BtuCD nor BtuCD-F have high affinity for substrate, regardless of their nucleotide state; accordingly, thermodynamic considerations (Fig 7a, horizontal bottom constants of panels I and IV) provide an estimate of 10<sup>-3</sup> M for the affinity between BtuCD-F and vitamin B<sub>12</sub>.

Upon association of vitamin B<sub>12</sub>-loaded BtuF and BtuCD, substrate is released from BtuF and is not retained by the complex (Fig 4, Fig. 7b state II). These findings are in agreement with the absence of vitamin B<sub>12</sub> from the published crystal structure of the BtuCD-F complex (despite that this complex was prepared by incubating vitamin B<sub>12</sub>-loaded BtuF with BtuCD<sup>16</sup>). Clearly, our present work could not determine the directionality of substrate release as these experiments were conducted in solution (Fig. 4). It is possible that in our solution experiments, vitamin B<sub>12</sub> is released at the *cis* side via an “escape pathway”, rather than being properly released at the *trans* side (productive transport). If indeed such escape pathway occurs, this may explain the poor transport stoichiometry (~100 ATP/ vitamin B<sub>12</sub>) measured in reconstituted proteoliposomes<sup>20</sup>.

The key findings of the present report are at variance from the mechanistic model that has been established in detail for the maltose transporter (Fig. 7b), and to varying degrees for other ABC transporters<sup>11,32</sup>. In the histidine and maltose import systems, substrate-free or substrate-loaded binding proteins interact with similar equilibrium affinity (micromolar range) with the transporter<sup>24,27</sup>. In the oligopeptide import system (OppABCDF), substrate greatly increases the affinity between the membrane embedded transporter and its receptor<sup>9</sup>. As reported here, a very different substrate effect is observed in the BtuCD-F system: vitamin B<sub>12</sub> accelerates complex formation 10-20-fold, and complex dissociation ~10<sup>7</sup>-fold, resulting in a ~10<sup>5</sup> drop in equilibrium affinity (Figs 5, 6 and 7, table I). The effects of vitamin B<sub>12</sub> on the kinetics of interaction between BtuCD and BtuF underline the importance of conducting pre-equilibrium measurements of ABC transport systems.

Another mechanistic aspect that seems to differ between ABC transporters is the effect of binding protein on the rate of ATP hydrolysis. In the maltose and the histidine systems, marked increase of ATPase rates is induced only by association of substrate-loaded binding protein with the transporter. In contrast, very modest stimulation (less than 2-fold<sup>20</sup>, supplementary Fig. 1) of ATP hydrolysis rate is observed upon formation of the BtuCD-F complex, and this low-level stimulation is conveyed by substrate-free and substrate-loaded binding protein alike. With the exception of the TAP system<sup>33,34</sup>, low levels of substrate-induced stimulation of ATPase rates also seem to be a feature of ABC exporters, especially multi-drug transporters<sup>35,37</sup>. The differences in substrate-induced effects on the interaction between the binding protein and the transporter (and its outcome) is perhaps related to the extent of substrate-induced conformational changes of the binding proteins: the maltose and histidine binding proteins (of type I ABC importers) undergo appreciable structural



rearrangements upon substrate binding<sup>38</sup>. In comparison, ShuT<sup>39</sup>, PhuT<sup>40</sup>, FhuD<sup>41</sup> and BtuF<sup>15, 42</sup> (binding proteins of type II ABC importers) exhibit modest to negligible conformational changes upon substrate binding.

BtuCD has the lowest affinity for BtuF in the ATP-bound or transition state analog-bound forms (Fig. 7a panels II & III, Fig. 7b state III, Fig 6, table I). In its nucleotide-free state, BtuCD has the highest affinity towards BtuF. Again, this is in direct opposition to the maltose system, where it was clearly demonstrated that the nucleotide bound transporter, and the transition state for ATP hydrolysis, have the highest affinity toward the maltose binding protein, while the nucleotide-free form has the lowest (Fig. 7b, state II of bottom panel)<sup>21</sup>. Similarly, following release of vitamin B<sub>12</sub>, the now substrate-free BtuCD-F complex represents the most stable, lowest energy state of the transport cycle (Fig. 7a panel I, bottom left corner). In comparison, the MalFGK-E complex is the highest energy intermediate of the reaction, and under normal turnover conditions it is undetectable. In this respect, the putative metal-chelate import system (Hi1470/1/2) resembles BtuCD-F, as it forms a quasi-stable complex in the absence of nucleotide (Fig 1b, Fig 2b&e), while the D/L-methionine import system (MetIN-Q) forms a low affinity complex (Fig 2c&f) much like MalFGK-E or HisPQM-J.

Sequence based phylogenetic segregation of ABC transporters divides them to distinct evolutionary branches<sup>18</sup>. According to this classification, BtuCD-F and Hi1470/1/2 are similar to each other, yet are relatively distant from the maltose, molybdate, histidine, and methionine import systems. In addition to sequence conservation, recent comparisons of the crystal structures of ABC transporters suggest that the phylogenetic groups may also share a common fold of their membrane-spanning domain<sup>5, 19</sup>. Thus, the maltose, molybdate, and methionine import systems share a core fold that is distinct from the fold shared by BtuCD-F and Hi1470/1-2. In the present report, we add another dimension to this picture, and suggest that members of different subclasses of ABC transporters differ not only in sequence and structure, but also in mechanism. Further investigations of the genetic, structural, and functional heterogeneity of ABC transporters will clearly advance our understanding of these elaborate cellular machines.

## Supplementary Material

Refer to Web version on PubMed Central for supplementary material.

## Acknowledgments

We thank Heather Pinkett for insightful discussions and critical reading of the manuscript, and Joshua Klein and Jost Vielmetter for their help in the initial BiaCore experiments. The work was supported in part by National Institutes of Health grant GM045162 and the Howard Hughes Medical Institute, and by fellowships to O.L. from the Fulbright Foundation and the Jane Coffin Childs Memorial Fund for Medical Research.

## Appendix

### Materials and Methods

#### Protein purifications

BtuCD, MetIN, and Hi1470/71 were purified as previously described<sup>43-45</sup>. BtuF and Hi1472 were expressed with a C-terminal FLAG tag and purified using anti-FLAG M2 agarose (Sigma) from osmotic shock extracts. MetQ was expressed with an N-terminal 10-His tag, and following purification, the tag was removed using EnteroKinase digestion according to the manufacturer's specifications (BioLabs). Protein samples were concentrated to 5-10 mg ml<sup>-1</sup> (Amicon Ultra concentrators, Millipore), snap frozen as small aliquots in liquid nitrogen, and stored in -80 °C for up to 3 months.

#### Reconstitution of BtuCD, MetIN and association experiments in liposomes

BtuCD was reconstituted essentially as previously described<sup>20</sup>, only that 0.1 % (W/V) LDAO (n-dodecyl-N, N-dimethylamine-N-oxide) was used throughout the purification and reconstitution process. MetIN was reconstituted in a similar fashion, only that 0.05 % (W/V) DDM (n-dodecyl- $\beta$ -maltopyranoside) was used throughout. For association experiments with BtuF, liposomes or proteoliposomes were re-suspended to a final concentration of 10 mg ml<sup>-1</sup> lipids and 0.075 mg ml<sup>-1</sup> protein in 50 mM Tris-HCl pH 7.5, 150 mM NaCl. FLAG-tagged BtuF was then added at the indicated concentrations (with additional additives where appropriate) and the suspension was tilted at 25°C for 10 minutes. The suspension was then spun for 20 minutes at 150,000g, the supernatant removed, and the pellet was re-suspended with an equal volume of buffer + 1% (W/V) SDS. The amount of BtuF present in each fraction was visualized by immunoblot detection (using an anti-FLAG antibody) following SDS-PAGE.

#### Size exclusion chromatography

100-200  $\mu$ l samples were injected to a Superdex<sup>TM</sup> 200 10/300 column (GE Healthcare) mounted on an AKTA purifier system. Absorbance was recorded at 280 nm or 360 nm as indicated. Excess vitamin B<sub>12</sub> was removed from BtuF by successive cycles, as indicated, of 10-fold dilutions (with buffer devoid of vitamin B<sub>12</sub>) and re-concentration using an Amicon Ultra concentrator (Millipore). Where applicable, 1 mM ATP, 50  $\mu$ M EDTA, or 1 mM ATP, 2 mM MgSO<sub>4</sub>, 1 mM ortho-vanadate, or 1 mM ADP, 2 mM MgSO<sub>4</sub>, or 1 mM ATP, 2 mM MgSO<sub>4</sub>, or 1 mM AMP-PCP, 2 mM MgSO<sub>4</sub>, or 1 mM AMP-PNP, 2 mM MgSO<sub>4</sub> where added to both the column buffer and to the injected sample.

#### Pull-down experiments

Purified, His-tagged BtuCD was immobilized onto a Ni-NTA resin (10  $\mu$ l per sample), followed by a washing step to remove unbound protein. 250  $\mu$ l of purified FLAG-tagged MetQ were added at the indicated concentrations. Following a 10-min incubation, unbound material was removed by applying vacuum to Qiagen's miniprep spin-columns. Six subsequent washes were used to insure complete removal of unbound protein. Where appropriate, nucleotides and/or substrate were included in the washing buffer. Bound material was then eluted in a single step with buffer (100  $\mu$ l) containing 1 M imidazole. The

amount of retained FLAG-tagged protein in the sample was visualized using standard immuno-blot procedures, using an anti-FLAG M2 HRP-conjugate antibody (Sigma).

### BiaCore™ measurements

For ligand and analyte preparations, great care was taken to remove all traces of aggregated material by using size exclusion chromatography and ultracentrifugation (270,000g, 20 min). BtuCD and Hi1470/71 were immobilized onto a Ni-NTA chip, and MetIN to a CM-5 chip via an anti-PentaHis antibody (Qiagen). Roughly 30 ng of the transporters were immobilized per flow-cell. All measurements were conducted at 25 °C, and the block compartment was cooled to 7-8 °C. Mass transport limitations were not observed with BtuCD-F or MetIN-Q, and experiments were conducted at a flow rate of 15 and 25  $\mu\text{l min}^{-1}$ , respectively. Due to the slightly higher rates of the Hi1470/71 system, 50  $\mu\text{l min}^{-1}$  was used. Experiments were run in 50 mM Tris-HCl pH 7.5, 150 mM NaCl, 0.1% (W/V) n-dodecyl-N, N-dimethylamine-N-oxide (LDAO) (BtuCD-F), 10 mM Hepes, 150 mM NaCl, 50  $\mu\text{M}$  EDTA, 0.05% (W/V) n-dodecyl- $\beta$ -maltopyranoside, pH 7.35 (MetIN-Q), or 25 mM Tris-Hcl pH 7.5, 500 mM NaCl, 0.2% (W/V) n-decyl- $\beta$ -maltopyranoside (Hi1470/1-2). Where appropriate, substrates and/or nucleotides were added only to the analyte's buffer. Data was collected on BiaCore™T100 or 2000 systems.

### Biacore data analysis and model fitting

All models used for fitting of the experimental data are part of the Biacore evaluation software. Despite the clear biphasic nature of the association curves, we initially attempted fitting by applying a simple one to one binding model. As expected, the statistics, and fit quality of these preliminary fits were poor. We then applied for each of the experiments shown a model that accounts for a possible conformational following complex formation  $A + B \leftrightarrow AB \leftrightarrow AB'$ , where A and B represent the transporter and binding protein. In this model,  $k_{a1}$  and  $k_{d1}$  are the forward and reverse rate constants for complex formation, while  $k_{a2}$  and  $k_{d2}$  are the forward and reverse rate constants for the conformational change. The overall dissociation constant for this scheme  $K_d$ , is related to the rate constants through the expression:

$$K_d = \frac{[A][B]}{[AB] + [AB']} = \frac{k_{d1}k_{d2}}{k_{a1}(k_{d2} + k_{a2})}$$

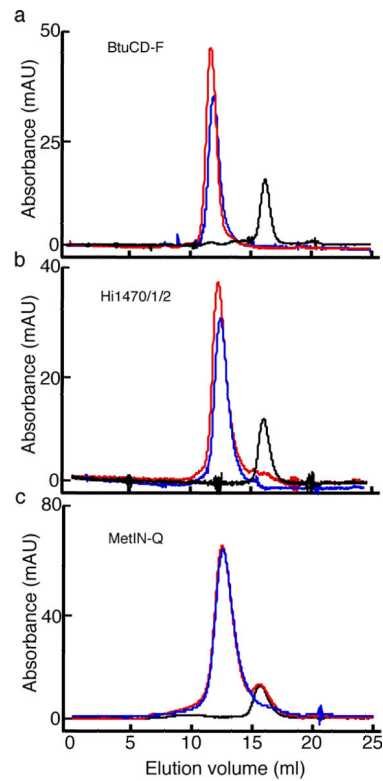
A more detailed description of the parameters and equations is provided in the BiaCore™ (GE Healthcare) T100 Software Handbook BR-1006-48, edition AE, pages 186-187.

### References

1. Higgins CF. ABC transporters: from microorganisms to man. *Annu Rev Cell Biol.* 1992; 8:67–113. [PubMed: 1282354]
2. Higgins CF. ABC transporters: physiology, structure and mechanism--an overview. *Res Microbiol.* 2001; 152:205–10. [PubMed: 11421269]
3. van der Does C, Tampe R. How do ABC transporters drive transport? *Biol Chem.* 2004; 385:927–33. [PubMed: 15551867]

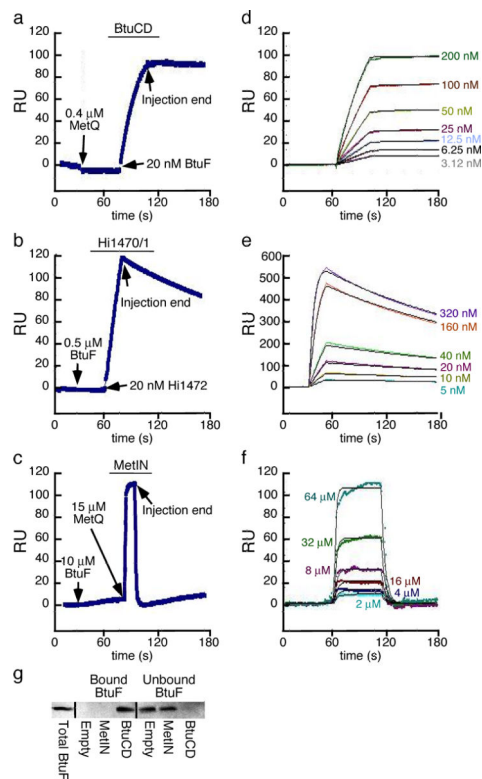
4. Davidson AL, Dassa E, Orelle C, Chen J. Structure, function, and evolution of bacterial ATP-binding cassette systems. *Microbiol. Mol. Biol. Rev.* 2008; 72:317–364. [PubMed: 18535149]
5. Locher KP. Review. Structure and mechanism of ATP-binding cassette transporters. *Philos Trans R Soc Lond B Biol Sci.* 2009; 364:239–45. [PubMed: 18957379]
6. Jones PM, O'Mara ML, George AM. ABC transporters: a riddle wrapped in a mystery inside an enigma. *Trends Biochem. Sci.* 2009; 34:520–531. [PubMed: 19748784]
7. Boos, W.; Lucht, JM. Periplasmic binding protein-dependent ABC transporters.. In: Neidhardt, FC., editor. *Escherichia coli and Salmonella typhimurium: Cellular and Molecular Biology*. Vol. 1. American Society for Microbiology; Washington, DC: 1996. p. 1175-1209.
8. Rohrbach MR, Braun V, Koster W. Ferrichrome transport in *Escherichia coli K-12*: altered substrate specificity of mutated periplasmic FhuD and interaction of FhuD with the integral membrane protein FhuB. *J Bacteriol.* 1995; 177:7186–93. [PubMed: 8522527]
9. Doeven MK, Abele R, Tampe R, Poolman B. The binding specificity of OppA determines the selectivity of the oligopeptide ATP-binding cassette transporter. *J Biol Chem.* 2004; 279:32301–7. [PubMed: 15169767]
10. Orelle C, Ayvaz T, Everly RM, Klug CS, Davidson AL. Both maltose-binding protein and ATP are required for nucleotide-binding domain closure in the intact maltose ABC transporter. *Proc. Natl. Acad. Sci. U.S.A.* 2008; 105:12837–12842. [PubMed: 18725638]
11. Oldham ML, Khare D, Quijcho FA, Davidson AL, Chen J. Crystal structure of a catalytic intermediate of the maltose transporter. *Nature.* 2007; 450:515–522. [PubMed: 18033289]
12. Bassford PJ Jr. Bradbeer C, Kadner RJ, Schnaitman CA. Transport of vitamin B<sub>12</sub> in tonB mutants of *Escherichia coli*. *J Bacteriol.* 1976; 128:242–7. [PubMed: 135755]
13. Bassford PJ Jr. Kadner RJ. Genetic analysis of components involved in vitamin B<sub>12</sub> uptake in *Escherichia coli*. *J Bacteriol.* 1977; 132:796–805. [PubMed: 336607]
14. Cadieux N, et al. Identification of the periplasmic cobalamin-binding protein BtuF of *Escherichia coli*. *J Bacteriol.* 2002; 184:706–17. [PubMed: 11790740]
15. Borths EL, Locher KP, Lee AT, Rees DC. The structure of *Escherichia coli* BtuF and binding to its cognate ATP binding cassette transporter. *Proc Natl Acad Sci U S A.* 2002; 99:16642–7. [PubMed: 12475936]
16. Hvorup RN, et al. Asymmetry in the structure of the ABC transporter binding protein complex BtuCD-BtuF. *Science.* 2007; 317:1387–1390. [PubMed: 17673622]
17. Goetz BA, Perozo E, Locher KP. Distinct gate conformations of the ABC transporter BtuCD revealed by electron spin resonance spectroscopy and chemical cross-linking. *FEBS Lett.* 2009; 583:266–70. [PubMed: 19101549]
18. Dassa E, Bouige E. The ABC of ABCs: a phylogenetic and functional classification of ABC systems in living organisms. *Res. Microbiol.* 2001; 152:211–229. [PubMed: 11421270]
19. Rees DC, Johnson E, Lewinson O. ABC transporters: the power to change. *Nat Rev Mol Cell Biol.* 2009; 10:218–27. [PubMed: 19234479]
20. Borths EL, Poolman B, Hvorup RN, Locher KP, Rees DC. In vitro functional characterization of BtuCD-F, the *Escherichia coli* ABC transporters for vitamin B<sub>12</sub> uptake. *Biochemistry.* 2005; 44:16301–16309. [PubMed: 16331991]
21. Chen J, Sharma S, Quijcho FA, Davidson AL. Trapping the transition state of an ATP-binding cassette transporter: evidence for a concerted mechanism of maltose transport. *Proc Natl Acad Sci U S A.* 2001; 98:1525–30. [PubMed: 11171984]
22. Liu CE, Ames GF. Characterization of transport through the periplasmic histidine permease using proteoliposomes reconstituted by dialysis. *J Biol Chem.* 1997; 272:859–66. [PubMed: 8995374]
23. Merino G, Boos W, Shuman HA, Bohl E. The inhibition of maltose transport by the unliganded form of the maltose-binding protein of *Escherichia coli*: experimental findings and mathematical treatment. *J Theor Biol.* 1995; 177:171–9. [PubMed: 8558904]
24. Ames GF, Liu CE, Joshi AK, Nikaido K. Liganded and unliganded receptors interact with equal affinity with the membrane complex of periplasmic permeases, a subfamily of traffic ATPases. *J Biol Chem.* 1996; 271:14264–70. [PubMed: 8662800]

25. van der Does C, Presenti C, Schulze K, Dinkelaker S, Tampe R. Kinetics of the ATP hydrolysis cycle of the nucleotide-binding domain of Mdl1 studied by a novel site-specific labeling technique. *J Biol Chem.* 2006; 281:5694–701. [PubMed: 16352609]
26. Pick U. The interaction of vanadate ions with the Ca-ATPase from sarcoplasmic reticulum. *J Biol Chem.* 1982; 257:6111–9. [PubMed: 6210692]
27. Austerhuhle MI, Hall JA, Klug CS, Davidson AL. Maltose-binding protein is open in the catalytic transition state for ATP hydrolysis during maltose transport. *J Biol Chem.* 2004; 279:28243–50. [PubMed: 15117946]
28. James KJ, Hancock MA, Gagnon JN, Coulton JW. TonB interacts with BtuF, the *Escherichia coli* periplasmic binding protein for cyanocobalamin. *Biochemistry.* 2009
29. Lundrigan MD, Koster W, Kadner RJ. Transcribed sequences of the *Escherichia coli* btuB gene control its expression and regulation by vitamin B<sub>12</sub>. *Proc Natl Acad Sci U S A.* 1991; 88:1479–83. [PubMed: 1847525]
30. Richter-Dahlfors AA, Ravnun S, Andersson DI. Vitamin B<sub>12</sub> repression of the cob operon in *Salmonella typhimurium*: translational control of the cbiA gene. *Mol Microbiol.* 1994; 13:541–53. [PubMed: 7527895]
31. Van Hove B, Staudenmaier H, Braun V. Novel two-component transmembrane transcription control: regulation of iron dicitrate transport in *Escherichia coli* K-12. *J Bacteriol.* 1990; 172:6749–58. [PubMed: 2254251]
32. Khare D, Oldham ML, Orelle C, Davidson AL, Chen J. Alternating access in maltose transporter mediated by rigid-body rotations. *Mol Cell.* 2009; 33:528–36. [PubMed: 19250913]
33. Gorbulev S, Abele R, Tampe R. Allosteric crosstalk between peptide-binding, transport, and ATP hydrolysis of the ABC transporter TAP. *Proc Natl Acad Sci U S A.* 2001; 98:3732–7. [PubMed: 11274390]
34. Herget M, et al. Purification and reconstitution of the antigen transport complex TAP: A prerequisite for determination of peptide stoichiometry and ATP hydrolysis. *J Biol Chem.* 2009
35. Chang XB, Hou YX, Riordan JR. ATPase activity of purified multidrug resistance-associated protein. *J Biol Chem.* 1997; 272:30962–8. [PubMed: 9388243]
36. Ozvegy C, Varadi A, Sarkadi B. Characterization of drug transport, ATP hydrolysis, and nucleotide trapping by the human ABCG2 multidrug transporter. Modulation of substrate specificity by a point mutation. *J Biol Chem.* 2002; 277:47980–90. [PubMed: 12374800]
37. Sauna ZE, Nandigama K, Ambudkar SV. Multidrug resistance protein 4 (ABCC4)-mediated ATP hydrolysis: effect of transport substrates and characterization of the post-hydrolysis transition state. *J Biol Chem.* 2004; 279:48855–64. [PubMed: 15364914]
38. Quijcho FA, Ledvina PS. Atomic structure and specificity of bacterial periplasmic receptors for active transport and chemotaxis: variation of common themes. *Mol Microbiol.* 1996; 20:17–25. [PubMed: 8861200]
39. Eakanunkul S, et al. Characterization of the periplasmic heme-binding protein shut from the heme uptake system of *Shigella dysenteriae*. *Biochemistry.* 2005; 44:13179–91. [PubMed: 16185086]
40. Ho WW, et al. Holo- and apo-bound structures of bacterial periplasmic heme-binding proteins. *J Biol Chem.* 2007; 282:35796–802. [PubMed: 17925389]
41. Clarke TE, Braun V, Winkelmann G, Tari LW, Vogel HJ. X-ray crystallographic structures of the *Escherichia coli* periplasmic protein FhuD bound to hydroxamate-type siderophores and the antibiotic albomycin. *J Biol Chem.* 2002; 277:13966–72. [PubMed: 11805094]
42. Karpowich NK, Huang HH, Smith PC, Hunt JF. Crystal structures of the BtuF periplasmic-binding protein for vitamin B<sub>12</sub> suggest a functionally important reduction in protein mobility upon ligand binding. *J Biol Chem.* 2003; 278:8429–34. [PubMed: 12468528]
43. Locher KP, Lee AT, Rees DC. The *E. coli* BtuCD structure: a framework for ABC transporter architecture and mechanism. *Science.* 2002; 296:1091–8. [PubMed: 12004122]
44. Pinkett HW, Lee AT, Lum P, Locher KP, Rees DC. An inward-facing conformation of a putative metal-chelate type ABC transporter. *Science.* 2007; 315:373–377. [PubMed: 17158291]
45. Kadaba NS, Kaiser JT, Johnson E, Lee A, Rees DC. The high-affinity *E. coli* methionine ABC transporter: structure and allosteric regulation. *Science.* 2008; 321:250–253. [PubMed: 18621668]

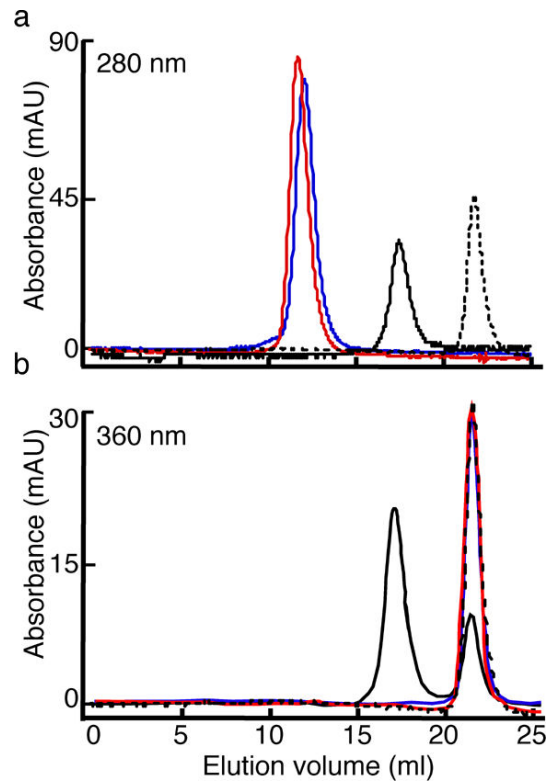


**Figure 1.**

Complex formation between ABC transporters and their binding proteins: (a) BtuCD-F (b) Hi1470/1-2 (c) MetIN-Q. Size exclusion chromatography of ABC transporters injected individually (blue traces) or after incubation with their binding proteins (red traces). Also shown are equi-molar injections of the binding proteins (black traces). Stable complex formation is characterized by a shift in the location of, and slight increase in area of the transporter peak, and by the disappearance of the binding protein peak. In (a) and (b), injections were at a 1:1 molar ratio (transporter:binding protein), in (c) 3:1 molar ratio.

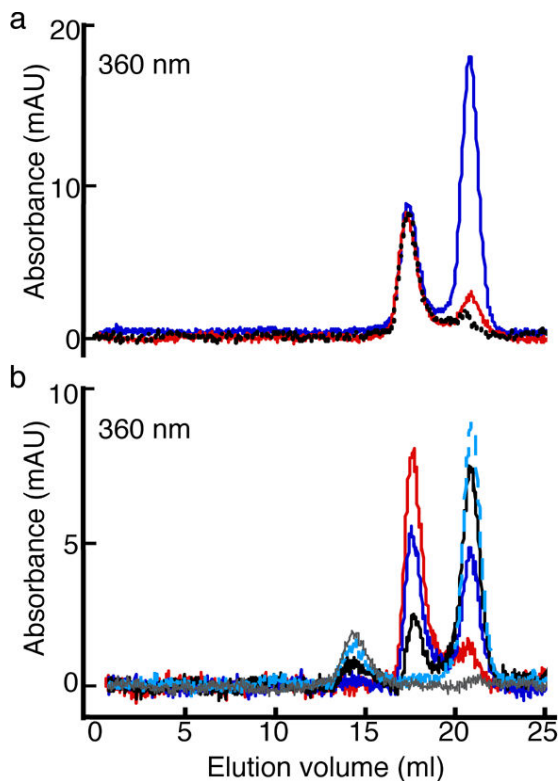


**Figure 2.** Dynamics of complex formation in BtuCD-F (a, d), Hi1470/1-2 (b, e), and MetIN-Q (c, f) import systems. The transporters (~30 ng) were immobilized onto a BiaCore™ chip and subjected to the following: (a, b, c) Injections of the BtuF, Hi1472, or MetQ as indicated by the arrows. (d, e, f) Injections of the indicated concentrations of BtuF, Hi1472, or MetQ, respectively. Black traces in d, e, and f are the fits to the experimental data curves. Standard errors for these fits are given in Table I. (g) Association of BtuF and BtuCD in proteoliposomes. 20 nM FLAG-tagged BtuF was added to empty liposomes or proteoliposomes reconstituted with either MetIN or BtuCD, as indicated. The liposome-bound and unbound fractions of BtuF were separated and visualized by immuno-blot detection.



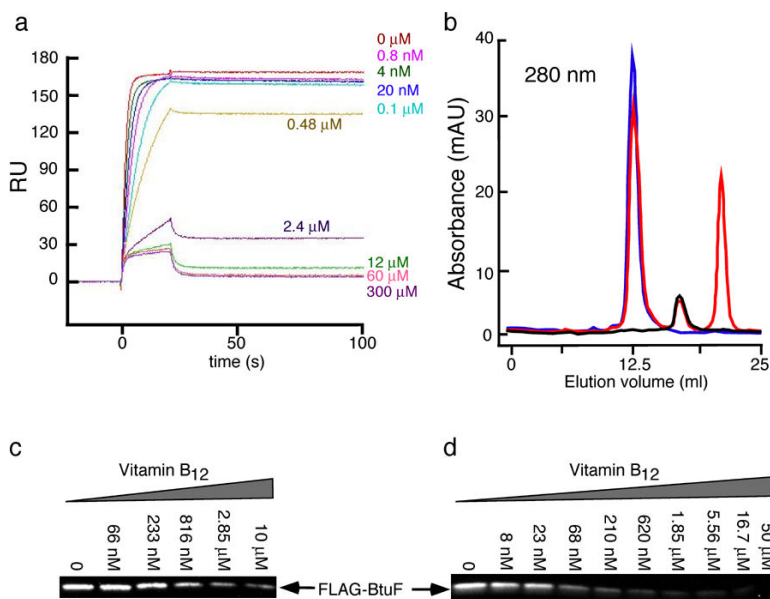
**Figure 3.** Substrate binding by components of the vitamin B<sub>12</sub> transport system. BtuCD (blue), BtuF (solid black), and the BtuCD-F complex (red) were purified and subjected to size exclusion chromatography before (a) or after (b) incubation with 50  $\mu$ M vitamin B<sub>12</sub> (dashed black). Absorbance was recorded at 280 nm (a) or 360 nm (b).



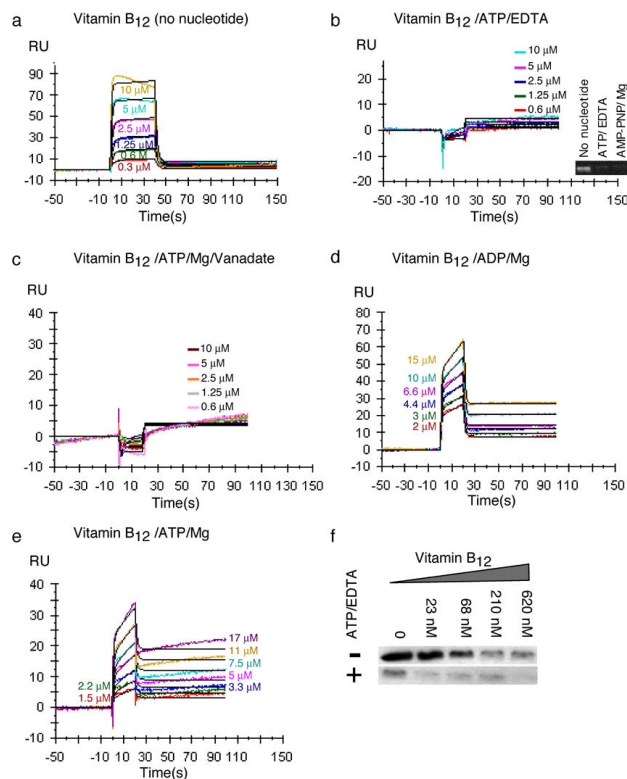


**Figure 4.**

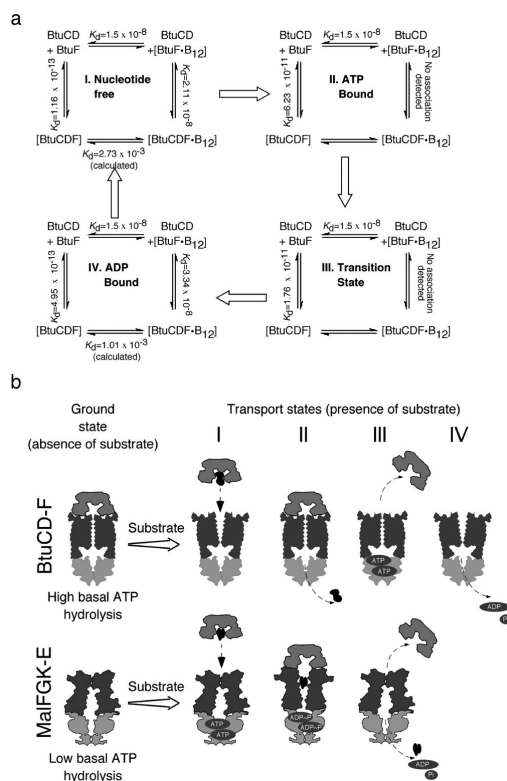
Substrate release from the vitamin B<sub>12</sub> transport system. (a) BtuF was prepared in the presence of 10  $\mu$ M vitamin B<sub>12</sub> and subjected to separation by size exclusion chromatography (blue). The same preparation was washed 10-fold (red) or 100-fold (dashed black) with buffer devoid of vitamin B<sub>12</sub>. Absorbance was recorded at 360 nm. (b) An identical preparation of BtuF (washed 100-fold) was subjected to separation by size exclusion chromatography before (red) or after incubation with BtuCD at 1:2 (blue), 1:1 (black), or 2:1 (dashed cyan) BtuCD:BtuF: molar ratio. Also shown (in grey) is an injection of BtuCD at the highest concentration used. Absorbance was recorded at 360 nm.



**Figure 5.** Substrate effects on complex formation in the vitamin B<sub>12</sub> transport system. (a) BiaCore™ experiments: His-tagged BtuCD (~30 ng) was immobilized onto a Ni-NTA chip. At 0 seconds, 1 μM BtuF was injected in the presence of 0-300 μM vitamin B<sub>12</sub>, as indicated. (b) Size exclusion chromatography: The following preparations were analyzed by gel filtration chromatography: BtuF prepared in the absence of vitamin B<sub>12</sub> and mixed with BtuCD (blue), BtuF prepared in the presence of 100 μM vitamin B<sub>12</sub> and then mixed with BtuCD (red). An identical amount of BtuF injected by itself (black). All traces were recorded at 280 nm. (c) Pull-down experiments: His-tagged BtuCD was immobilized onto Ni-NTA resin and incubated with 2 μM FLAG-BtuF in the absence or presence of the indicated vitamin B<sub>12</sub> concentrations. Unbound protein was removed, and the amount of retained FLAG-BtuF was visualized by immuno-detection using an anti-FLAG antibody. (d) Complex formation in proteoliposomes. 35 nM FLAG-tagged BtuF was added to BtuCD-proteoliposomes, in the absence or presence of the indicated vitamin B<sub>12</sub> concentrations. Bound and unbound BtuF were separated as detailed in the methods section. The amount of FLAG-BtuF was visualized by immuno-detection using an anti-FLAG antibody.

**Figure 6.**

Effects of nucleotide binding and hydrolysis on complex formation in the vitamin B<sub>12</sub> transport system. The indicated BtuF concentrations were injected in the presence of 200 μM vitamin B<sub>12</sub> and: (a) No further addition (b) 1 mM ATP, 50 μM EDTA (c) 1 mM ATP, 2 mM MgSO<sub>4</sub>, 1 mM ortho-vanadate (d) 1 mM ADP, 2 mM MgSO<sub>4</sub> (e) 1 mM ATP, 2 mM MgSO<sub>4</sub>. Black traces are the fits to the experimental data curves. Standard errors for these fits are given in Table I. Inset in (b) shows pull-down experiment of Ni-NTA-immobilized His-tagged BtuCD incubated with FLAG-tagged BtuF in the presence of 25 μM vitamin B<sub>12</sub>, in the absence of nucleotide, or in the presence of 1 mM ATP, 50 μM EDTA or 1 mM AMP-PNP, 2 mM MgSO<sub>4</sub> as indicated. The amount of retained FLAG-BtuF was visualized by immuno-detection using an anti-FLAG antibody. (f) Interaction in the membrane: BtuCD-liposomes were prepared in the absence (top panel) or presence (bottom panel) of 1 mM ATP, 50 μM EDTA. 35 nM FLAG-tagged BtuF was added to the liposomes in the presence of the indicated vitamin B<sub>12</sub> concentrations. Bound and unbound BtuF were separated as detailed in the methods section. The amount of FLAG-BtuF was visualized by immuno-detection using an anti-FLAG antibody.

**Figure 7.**

(a) Thermodynamic scheme summarizing the equilibrium constants determined for the vitamin B<sub>12</sub> transport system. Each panel represents a different nucleotide state of BtuCD: the horizontal reactions describe vitamin B<sub>12</sub> binding/release while the vertical reactions are for formation/dissociation of the BtuCD-F complex. In each panel, the vertical left and right reactions are for BtuCD-F complex formation in the absence and presence of vitamin B<sub>12</sub>, respectively. Unless otherwise indicated, all values were experimentally determined. (b) Mechanistic differences between the maltose transporter and BtuCD-F. The ground state of the vitamin B<sub>12</sub> system is the stable BtuCD-F complex, which has high levels of basal ATPase activity. In the maltose system, the corresponding state is that of the free transporter, with low levels of ATPase activity. In both systems the transition to the transport states is driven by substrate. Vitamin B<sub>12</sub> drives complex dissociation, while maltose, by stabilizing the closed conformation of MalE, contributes to complex stability. The MalFGK-E complex is stabilized by ATP binding (or transition state, panel II), while the BtuCD-F complex is destabilized by ATP binding (panel III).

Table 1

Kinetic rate constants determined in BiaCore™ experiments for the BtuCD-F, Hii1470/1-2, and MetIN-Q import systems.

Transport system	Additives	$k_{ad} \text{ M}^{-1} \text{ s}^{-1}$	$k_{d1} \text{ s}^{-1}$	$k_{d2} \text{ s}^{-1}$	$k_{d2} \text{ s}^{-1}$	$K_d \text{ (M)}$
Vitamin B <sub>12</sub>	None	$(4.54 \pm 0.05) \cdot 10^4$	$(1.12 \pm 0.28) \cdot 10^{-8}$	$(1.12 \pm 0.06) \cdot 10^{-3}$	$(9.95 \pm 0.18) \cdot 10^{-4}$	$1.16 \cdot 10^{-13}$
	Vitamin B <sub>12</sub>	$(3.85 \pm 0.15) \cdot 10^5$	$1.51 \pm 0.05$	$(2.37 \pm 0.02) \cdot 10^{-3}$	$(1.28 \pm 0.37) \cdot 10^{-5}$	$2.11 \cdot 10^{-8}$
	ATP/EDTA	$(9.58 \pm 0.07) \cdot 10^3$	$(1.36 \pm 0.09) \cdot 10^{-6}$	$(1.67 \pm 0.39) \cdot 10^{-3}$	$(9.79 \pm 0.38) \cdot 10^{-4}$	$6.23 \cdot 10^{-11}$
	ATP/EDTA + Vitamin B <sub>12</sub>	No association detected				
	ATP/Mg/vanadate	$(5.51 \pm 0.22) \cdot 10^4$	$(2.03 \pm 0.19) \cdot 10^{-6}$	$(1.01 \pm 0.09) \cdot 10^{-3}$	$(9.97 \pm 0.84) \cdot 10^{-5}$	$1.76 \cdot 10^{-11}$
Putative Metal-Chelate	ATP/Mg/vanadate + Vitamin B <sub>12</sub>	No association detected				
	ADP/Mg	$(4.82 \pm 0.06) \cdot 10^5$	$(3.01 \pm 0.01) \cdot 10^{-4}$	$(2.06 \pm 0.05) \cdot 10^{-2}$	$(5.2 \pm 0.21) \cdot 10^{-4}$	$4.95 \cdot 10^{-13}$
	ADP/Mg + Vitamin B <sub>12</sub>	$(2.10 \pm 0.04) \cdot 10^4$	$0.99 \pm 0.01$	$(2.02 \pm 0.03) \cdot 10^{-2}$	$(1.59 \pm 0.52) \cdot 10^{-5}$	$3.34 \cdot 10^{-8}$
D/L-methionine	ATP/Mg + Vitamin B <sub>12</sub>	$(3.73 \pm 0.00) \cdot 10^4$	$0.77 \pm 0.01$	$(5.14 \pm 0.01) \cdot 10^{-2}$	$(9.02 \pm 7.3) \cdot 10^{-6}$	$3.6 \cdot 10^{-9}$
	None	$(8.83 \pm 0.07) \cdot 10^5$	$(1.01 \pm 0.06) \cdot 10^{-2}$	$(4.55 \pm 0.41) \cdot 10^{-2}$	$(4.01 \pm 0.08) \cdot 10^{-2}$	$5.72 \cdot 10^{-9}$
	None	$(3.08 \pm 0.20) \cdot 10^3$	$0.23 \pm 0.04$	$(9.55 \pm 0.40) \cdot 10^{-7}$	$(9.00 \pm 3.00) \cdot 10^{-2}$	$7.40 \cdot 10^{-5}$

$k_{ad}$ ,  $k_{d1}$ ,  $k_{d2}$ : Forward and reverse rate constants of the initial association leading to complex formation.

$k_{d2}$ ,  $k_{d2}$ : Forward and reverse rate constants of the conformational change following complex formation.

$K_d$ : Dissociation constant calculated from derived rate constants (see Methods)